

Ab initio molecular dynamics calculations with simple, localized, orthonormal real-space basis sets

Yi Liu and Dawn A. Yarne

Department of Chemistry, New York University, New York, New York 10003, USA

Mark E. Tuckerman

Department of Chemistry and Courant Institute of Mathematical Sciences, New York University, New York, New York 10003, USA

(Received 17 May 2003; revised manuscript received 14 July 2003; published 29 September 2003)

Ab initio molecular dynamics, in which finite temperature molecular dynamics is performed with forces obtained from “on the fly” electronic structure calculations, is one of the most widely used theoretical tools for studying chemically active systems. Here, a significant step is taken to improve the efficiency, scaling with system size, and parallel efficiency of these calculations by the use of simple, localized, orthonormal real-space basis functions in conjunction with a unified reciprocal-space treatment of long-range interactions for various boundary conditions. This approach, which is capable of treating systems with zero-, one-, two-, or three-dimensional periodicity within a single framework, is shown to improve the convergence of total energies and forces by over an order of magnitude in grid size compared to the more commonly used plane-wave basis. Possibilities for employing the approach in a linear scaling method are briefly discussed.

DOI: 10.1103/PhysRevB.68.125110

PACS number(s): 71.15.Ap, 71.15.Mb, 71.15.Pd

I. INTRODUCTION

Since its introduction, *ab initio* molecular dynamics (AIMD),^{1–6} the marriage of electronic structure calculations and finite temperature molecular dynamics, has become one of the most powerful and widely used tools for studying the dynamics of a wide variety of chemical processes in both the liquid and solid states. Moreover, its recent combination with empirical force field methods,^{7–13} the so-called quantum mechanical/molecular mechanical or QM/MM approach, promises to yield schemes capable of treating large-scale systems with locally chemically active regions, opening new doors in the study of biological and industrial catalytic processes.

The original formulation of AIMD by Car and Parrinello,¹ involving a density functional theory (DFT) representation of the electronic structure combined with a plane-wave (PW) basis set expansion of the electronic orbitals, is still the mostly commonly used approach. Although elegant and conceptually simple, PW basis sets have the disadvantage of scaling as $O(N^2M)$, where N is the number of occupied electronic states, and M is the number of basis functions. In addition, PW's are not optimal for massively parallel computations due to the high communication overhead. In order to ameliorate these problems, localized real-space approaches,^{14–29} employing Gaussian basis sets,^{15,26} hybrid Gaussian/plane-wave basis sets,^{22–24} grid discretization schemes,^{17–20,25,27,28} and finite element methods,^{14,16,21} have been introduced. Gaussian bases, while highly popular, suffer from basis set superposition error and other complexities due to the nonorthogonality and position dependence of the functions. Grid discretization schemes are sensitive to the accuracy of the finite-difference approximation to the gradient and Laplacian operators.

In this paper, a simple, rigorous, orthonormal real space basis set method, which is free of the above difficulties, is combined with a unified reciprocal-space treatment of long-range interactions for cluster, wire, surface, and solid bound-

ary conditions in order to improve the scaling with system size, efficiency, and parallel scalability of AIMD calculations. The approach is based on the use of continuous functions that satisfy the properties of position eigenfunctions on an appropriately defined auxiliary grid. Such functions, originally introduced by Light and co-workers, are referred to as *discrete variable representations* (DVR's).^{30–41} The principal advantage of a DVR is the highly localized character of the basis functions about the points of the auxiliary grid. Thus, only a small number of functions is required to represent a spatially localized electronic orbital. This fact renders DVR's particularly useful for chemical applications and massively parallel computations. When combined with an orbital localization scheme, the use of DVR's leads to an $O(N)$ scaling method.^{42–51} Moreover, DVR's offer a good deal of flexibility in the particular choice of basis functions,^{34,37–41} which allows different types of boundary conditions (cluster, wire, surface, or solid) to be treated exactly and allows basis functions to be tailored to a specific problem using, for example, schemes proposed by Bačić and Light.⁵² Finally, for a given choice of DVR, electronic orbitals and density are defined everywhere in space (not just at grid points), so that exact representations of the Laplacian and gradient operators are available. Here, we shall show how one particular type of DVR, the direct-product DVR, yields a highly effective approach to AIMD calculations.

The organization of this paper is as follows: In Sec. II, the basic principles underlying the DVR approach and its implementation in the DFT-based electronic structure and AIMD methods are reviewed. This discussion includes a brief outline of the recently introduced screening function approach to cluster, wire, and surface calculations.^{53–55} Following this, a number of test systems are presented in Sec. III, which demonstrate the improved convergence of total energies and forces in the DVR approach as well as its parallel scaling and adiabaticity in Car-Parrinello molecular dynamics. Conclusions and future directions are given in Sec. IV.

II. METHODOLOGY

A one-dimensional DVR is defined by a set of $N L^2$ integrable functions, $\{u_i(x)\}, i=1, \dots, N$, a set of N grid points, $\{x_i\}$ and a set of weights, $\{|a_i|^2=w_i\}$ such that the basis functions satisfy the property

$$u_i(x_j) = \frac{\delta_{ij}}{a_i} \quad (1)$$

at each grid point. From Eq. (1) follow the orthogonality and completeness relations:

$$\sum_k |a_k|^2 u_i^*(x_k) u_j(x_k) = \delta_{ij}, \quad (2)$$

$$\sum_k |a_k|^2 u_k^*(x_i) u_k(x_j) = \delta_{ij}.$$

Therefore, any function, $f(x)$, can be expanded in terms of the DVR basis functions according to

$$f(x) = \sum_i c_i u_i(x), \quad (3)$$

where $c_i = a_i f(x_i)$. Finally, given a set of $N L^2$ orthonormal functions, $\{\phi_n(x)\}$, a DVR can be obtained from these according the construction rule:

$$u_i(x) = c_i^* \sum_{n=1}^N \phi_n^*(x_i) \phi_n(x), \quad (4)$$

which can be easily shown to satisfy the aforementioned requirements in Eqs. (1) and (2).

An important property of DVR's is that a projection operator

$$\mathcal{P}_N = \sum_{i=1}^N |u_i\rangle\langle u_i| \quad (5)$$

applied to any position-dependent operator, $\Omega(x)$ via

$$\tilde{\Omega}(x) = \mathcal{P}_N \Omega(x) \mathcal{P}_N \quad (6)$$

yields a diagonal operator in the DVR basis, i.e.,

$$\langle u_j | \tilde{\Omega}(x) | u_i \rangle = \omega(x_j) \delta_{ij}, \quad (7)$$

where $\omega(x)$ is the corresponding eigenvalue of $\Omega(x)$. As the basis set size approaches infinity, $\tilde{\Omega}(x)$, itself, becomes exactly diagonal, i.e.,

$$\lim_{N \rightarrow \infty} \langle u_j | \tilde{\Omega}(x) | u_i \rangle = \lim_{N \rightarrow \infty} \omega(x_j) \delta_{ij} \quad (8)$$

and $u_i(x)$ approaches an exact position eigenfunction. For finite N , $\tilde{\Omega}(x)$ is approximately diagonal in the DVR basis, i.e., $\langle u_j | \tilde{\Omega}(x) | u_i \rangle \approx \omega(x_j) \delta_{ij}$.

In order to develop a DVR-based approach to density functional electronic structure and *ab initio* molecular dynamics (MD) calculations, we begin with the expression for the total energy in the Kohn-Sham formulation:

$$\begin{aligned} E[\{\psi\}, \{\mathbf{R}\}] = & -\frac{1}{2} \sum_l \langle \psi_l | \nabla^2 | \psi_l \rangle + \frac{1}{2} \int d\mathbf{r} d\mathbf{r}' \frac{n(\mathbf{r})n(\mathbf{r}')}{|\mathbf{r}-\mathbf{r}'|} \\ & + E_{\text{xc}}[n] + E_{\text{loc}}[n, \{\mathbf{R}\}] + E_{\text{NL}}[\{\psi\}, \{\mathbf{R}\}] \\ & + U_{\text{ion-ion}}(\{\mathbf{R}\}) \end{aligned} \quad (9)$$

where $\{\mathbf{R}\}$ is a set of nuclear positions, $\{\psi\}$ is a set of n_{occ} electronic orbitals, required to satisfy the orthogonality relation $\langle \psi_l | \psi_m \rangle = \delta_{lm}$, $n(\mathbf{r})$ is the electronic density,

$$n(\mathbf{r}) = \sum_{l=1}^{n_{\text{occ}}} f_l |\psi_l(\mathbf{r})|^2, \quad (10)$$

where f_l is the occupation number of $|\psi_l\rangle$. In Eq. (9), $E_{\text{xc}}[n]$ is the exchange and correlation functional, and $E_{\text{loc}}[n, \{\mathbf{R}\}]$ and $E_{\text{NL}}[\{\psi\}, \{\mathbf{R}\}]$ are the local and nonlocal components of the external interaction, assumed to be described by a norm-conserving atomic pseudopotential.^{56,57} A DVR basis for expansion of the Kohn-Sham orbitals is constructed as a direct product of one-dimensional DVR's,

$$\Phi_{ijk}(\mathbf{r}) = u_i(x) v_j(y) w_k(z), \quad (11)$$

such that

$$\psi_i(\mathbf{r}) = \sum_{i,j,k} C_{ijk}^l \Phi_{ijk}(\mathbf{r}), \quad (12)$$

where C_{ijk}^l is a set of expansion coefficients. Since the basis functions do not depend on atomic positions, the Hellman-Feynman theorem may be employed to obtain interatomic forces. Note that the functions u_i , v_j , and w_k need not be constructed from the same finite basis representation, a fact that can be exploited to treat different boundary conditions. For example, in order to treat a periodic dimension of length L , a DVR constructed via

$$u_i^{(\text{per})}(x) = \sqrt{\frac{1}{NL}} \sum_{\alpha=1}^N \cos[k_\alpha(x-x_i)], \quad (13)$$

where $k_\alpha = 2\pi(\alpha - N' - 1)/L$, $\alpha = 1, 2, \dots, N = 2N' + 1$ could be employed, while a nonperiodic dimension could be treated by a fixed-node DVR of the form

$$u_i^{(\text{clus})}(x) = \frac{2}{\sqrt{(N+1)L}} \sum_{\beta=1}^N \sin k_\beta x \sin k_\beta x_i, \quad (14)$$

where $k_\beta = \pi\beta/L$, $\beta = 1, 2, \dots, N$. Thus, solids or liquids could be treated by employing $u^{(\text{per})}$ in all three dimensions, surfaces treated by $u^{(\text{clus})}$ in one dimension, and $u^{(\text{per})}$ in two dimensions, etc. Indeed, DVRs offer considerable flexibility, permitting the construction of DVR's for a wide variety of purposes.^{34,37-41}

In the DVR basis, the orbitals are defined everywhere in space, not just at grid points. Thus, each term in Eq. (9) has a well-defined expression. For a direct-product DVR, the kinetic energy takes the form

$$T = -\frac{1}{2} \sum_l \sum_{i,i'} \sum_{j,j'} \sum_{k,k'} C_{ijk}^l T_{ii',jj',kk'} C_{i'j'k'}^l, \quad (15)$$

where the matrix $T_{ii',jj',kk'}$ has the general highly sparse form

$$T_{ii',jj',kk'} = t_{ii'}^x \delta_{jj'} \delta_{kk'} + t_{jj'}^y \delta_{ii'} \delta_{kk'} + t_{kk'}^z \delta_{ii'} \delta_{jj'}. \quad (16)$$

For the DVR's in Eqs. (13) and (14), the matrix $t_{nn'}^\gamma$, $\gamma = x, y, z$, can be worked out analytically and is given by³⁵

$$t_{nn'}^\gamma = - \left(\frac{2\pi}{L_\gamma} \right)^2 \frac{N'}{3} (N' + 1) \delta_{nn'} - \frac{(2\pi/L_\gamma)^2 (-1)^{n-n'} \cos[\pi(n-n')/N]}{2 \sin^2[\pi(n-n')/N]} (1 - \delta_{nn'}) \quad (17)$$

for the periodic and

$$t_{nn'}^\gamma = - \frac{1}{L_\gamma^2} \frac{\pi^2}{2} \left[\frac{2(N+1)^2 + 1}{3} - \frac{1}{\sin^2[\pi n/(N+1)]} \right] \delta_{nn'} - \frac{(-1)^{n-n'}}{L_\gamma^2} \frac{\pi^2}{2} \left[\frac{1}{\sin^2[\pi(n-n')/2(N+1)]} - \frac{1}{\sin^2[\pi(n+n')/2(N+1)]} \right] (1 - \delta_{nn'}) \quad (18)$$

for the fixed-node DVR's, Eqs. (13) and (14), respectively. Here L_γ is the length of the cell in the γ direction. Unlike in standard finite-difference schemes, the kinetic energy is exact for a given DVR and is appropriately matched to the boundary conditions.

In order to evaluate density-dependent terms, one begins with the fact that

$$n(\mathbf{r}) = \sum_{l=1}^{n_{\text{occ}}} f_l \left| \sum_{i,j,k} C_{ijk}^l \Phi_{ijk}(\mathbf{r}) \right|^2 \quad (19)$$

from which a set of DVR density coefficients, $N_{ijk} = (\sum_l f_l C_{ijk}^l)^2 / (|a_i|^2 |a_j|^2 |a_k|^2)$ may be computed. When generalized gradient functionals are employed, which require $\nabla n(\mathbf{r})$, a simple, exact expression for the latter is available for a given DVR by direct differentiation of Eq. (19). For example, the x component of the gradient, $n_x = \partial n / \partial x$, at a grid point $\mathbf{r}_{ijk} = (x_i, y_k, z_k)$ is given by

$$n_x(\mathbf{r}_{ijk}) = \sum_l f_l \left[\frac{1}{a_i^* w_j w_k} C_{ijk}^{l*} \sum_{i'} C_{i'jk}^l u_{i'}'(x_i) + \frac{1}{a_i w_j w_k} C_{ijk}^l \sum_{i'} C_{i'jk}^{l*} u_{i'}'^*(x_i) \right], \quad (20)$$

with analogous expressions for the y and z components. Equation (20) shows that the gradient of the density involves derivatives of the DVR basis functions at grid points, which may be computed once at the beginning of a calculation and stored. Since E_{xc} is evaluated on a grid, a real-space version of the scheme introduced by White and Bird⁵⁸ can be employed.

The long-range Hartree and local pseudopotential energies can either be evaluated in real space using fast multipole methods^{59,60} or in reciprocal space, as is employed here. Thus, long-range energies can be evaluated efficiently and simply with a single Fast Fourier transform (FFT), while the electronic gradient requires only one additional FFT. The long-range component of the local pseudopotential energy for the I th nucleus is assumed to be of the form $-Z_I \text{erf}(\beta|\mathbf{r}-\mathbf{R}_I|)/|\mathbf{r}-\mathbf{R}_I|$, where Z_I is the valence charge. In order to treat different boundary conditions, the reciprocal-space screening function approach recently pioneered by Martyna, Tuckerman, and co-workers is combined with the DVR basis approach.^{53-55,66} In the following, we briefly review this approach. In the screening function method, interaction potentials in nonperiodic systems are separated into short- and long-range contributions, and the latter are evaluated using a first-image approximation along the nonperiodic spatial directions in place of the usual supercell approach. In this way, the error can be controlled by the dimension of the simulation cell. Thus, given any density, $n(\mathbf{r})$, and any interaction potential, $\phi(\mathbf{r}-\mathbf{r}')$, the average potential energy in this approximation is given by

$$\langle \phi \rangle^{(1)} = \frac{1}{2V} \sum_{\mathbf{g}} |n_{\mathbf{g}}|^2 \bar{\phi}(-\mathbf{g}), \quad (21)$$

where V is the volume of the cell, and $\bar{\phi}(\mathbf{g})$ is a Fourier expansion coefficient of the potential given by

$$\begin{aligned} \bar{\phi}(\mathbf{g}) &= \int_{-L_c/2}^{L_c/2} dz \int_{-L_b/2}^{L_b/2} dy \int_{-L_a/2}^{L_a/2} dx \phi(\mathbf{r}) e^{-i\mathbf{g}\cdot\mathbf{r}} \quad (\text{cluster}), \\ \bar{\phi}(\mathbf{g}) &= \int_{-L_c/2}^{L_c/2} dz \int_{-L_b/2}^{L_b/2} dy \int_{-\infty}^{\infty} dx \phi(\mathbf{r}) e^{-i\mathbf{g}\cdot\mathbf{r}} \quad (\text{wire}), \\ \bar{\phi}(\mathbf{g}) &= \int_{-L_c/2}^{L_c/2} dz \int_{-\infty}^{\infty} dy \int_{-\infty}^{\infty} dx \phi(\mathbf{r}) e^{-i\mathbf{g}\cdot\mathbf{r}} \quad (\text{surface}). \end{aligned} \quad (22)$$

Here, L_a , L_b , and L_c are the dimensions of the simulation cell (assumed to be orthorhombic for simplicity) in the x , y , and z directions. [Note that the $\mathbf{g}=(0,0,0)$ term is not excluded.] In order to have an expression that is easily computed within the plane-wave description, consider two functions $\phi^{(\text{long})}(\mathbf{r})$ and $\phi^{(\text{short})}(\mathbf{r})$, which are taken to be the long- and short-range contributions to the total potential, i.e.,

$$\phi(\mathbf{r}) = \phi^{(\text{long})}(\mathbf{r}) + \phi^{(\text{short})}(\mathbf{r}),$$

$$\bar{\phi}(\mathbf{g}) = \bar{\phi}^{(\text{long})}(\mathbf{g}) + \bar{\phi}^{(\text{short})}(\mathbf{g}). \quad (23)$$

We require that $\phi^{(\text{short})}(\mathbf{r})$ vanish exponentially quickly at large distances from the center of the cell and that $\phi^{(\text{long})}(\mathbf{r})$ contain the long-range dependence of the full potential, $\phi(\mathbf{r})$. With these two requirements, it is possible to write

$$\begin{aligned}
 \bar{\phi}^{(\text{short})}(\mathbf{g}) &= \int_{D(V)} d\mathbf{r} \exp(-i\mathbf{g}\cdot\mathbf{r}) \phi^{(\text{short})}(\mathbf{r}) \\
 &= \int_{\text{all space}} d\mathbf{r} \exp(-i\mathbf{g}\cdot\mathbf{r}) \phi^{(\text{short})}(\mathbf{r}) + \epsilon(\mathbf{g}) \\
 &= \bar{\phi}^{(\text{short})}(\mathbf{g}) + \epsilon(\mathbf{g}), \tag{24}
 \end{aligned}$$

with exponentially small error, $\epsilon(\mathbf{g})$, provided the range of $\phi^{(\text{short})}(\mathbf{r})$ is small compared to the size of the parallelepiped. In order to ensure that Eq. (24) is satisfied, a convergence parameter, α , is introduced, which can be used to adjust the range of $\phi^{(\text{short})}(\mathbf{r})$ such that $\epsilon(\mathbf{g}) \sim 0$ and the error, $\epsilon(\mathbf{g})$, will be neglected in the following.

The function, $\bar{\phi}^{(\text{short})}(\mathbf{g})$, is the Fourier transform of $\phi^{(\text{short})}(\mathbf{r})$. Therefore,

$$\begin{aligned}
 \bar{\phi}(\mathbf{g}) &= \bar{\phi}^{(\text{long})}(\mathbf{g}) + \bar{\phi}^{(\text{short})}(\mathbf{g}) = \bar{\phi}^{(\text{long})}(\mathbf{g}) - \bar{\phi}^{(\text{long})}(\mathbf{g}) \\
 &+ \bar{\phi}^{(\text{short})}(\mathbf{g}) + \bar{\phi}^{(\text{long})}(\mathbf{g}) = \hat{\phi}^{(\text{screen})}(\mathbf{g}) + \bar{\phi}(\mathbf{g}), \tag{25}
 \end{aligned}$$

where $\bar{\phi}(\mathbf{g}) = \bar{\phi}^{(\text{short})}(\mathbf{g}) + \bar{\phi}^{(\text{long})}(\mathbf{g})$ is the Fourier transform of the full potential, $\phi(\mathbf{r}) = \phi^{(\text{short})}(\mathbf{r}) + \phi^{(\text{long})}(\mathbf{r})$ and

$$\hat{\phi}^{(\text{screen})}(\mathbf{g}) = \bar{\phi}^{(\text{long})}(\mathbf{g}) - \bar{\phi}^{(\text{long})}(\mathbf{g}). \tag{26}$$

Thus, Eq. (26) becomes leads to

$$\langle \phi \rangle = \frac{1}{2V} \sum_{\mathbf{g}} |\bar{n}(\mathbf{g})|^2 [\bar{\phi}(-\mathbf{g}) + \hat{\phi}^{(\text{screen})}(-\mathbf{g})]. \tag{27}$$

The new function appearing in the average potential energy, Eq. (27), is the difference between the Fourier series and Fourier transform form of the long-range part of the potential energy and will be referred to as the screening function because it is constructed to “screen” the interaction of the system with an infinite array of periodic images. The Coulomb potential, $\phi(\mathbf{r}) = 1/r$, can be separated into short- and long-range components via

$$\frac{1}{r} = \frac{\text{erf}(\alpha r)}{r} + \frac{\text{erfc}(\alpha r)}{r}, \tag{28}$$

where α is an arbitrary parameter. In Eq. (28), the first term is long range. The screening function for the cluster case is easily computed by introducing an FFT grid and performing the integration numerically.⁵³ For the wire⁵⁵ and surface⁵⁴ cases, analytical expressions can be worked out and are given by

$$\begin{aligned}
 \bar{\phi}^{(\text{screen})}(\mathbf{g}) &= -\frac{4\pi}{g^2} \left\{ \cos\left(\frac{g_c L_c}{2}\right) \left[\exp\left(-\frac{g_s L_c}{2}\right) \right. \right. \\
 &- \frac{1}{2} \exp\left(-\frac{g_s L_c}{2}\right) \text{erfc}\left(\frac{\alpha^2 L_c - g_s}{2\alpha}\right) - \frac{1}{2} \exp \\
 &\times \left(\frac{g_s L_c}{2}\right) \text{erfc}\left(\frac{\alpha^2 L_c + g_s}{2\alpha}\right) \left. \right] + \exp\left(-\frac{g^2}{4\alpha^2}\right) \\
 &\times \text{Re}\left[\text{erfc}\left(\frac{\alpha^2 L_c + i g_c}{2\alpha}\right)\right] \left. \right\} \quad (\text{surface}), \tag{29}
 \end{aligned}$$

$$\begin{aligned}
 \bar{\phi}^{(\text{screen})}(\mathbf{g}) &= \frac{4\pi}{g^2} \left[\exp(-g^2/4\alpha^2) E(\alpha, L_b, g_b) E(\alpha, L_c, g_c) \right. \\
 &+ \cos\left(\frac{g_b L_b}{2}\right) \frac{4\sqrt{\pi}}{\alpha L_b} \\
 &\times \exp(-g_c^2/4\alpha^2) I(\alpha, L_b, L_c, g_c) \\
 &+ \cos\left(\frac{g_c L_c}{2}\right) \frac{4\sqrt{\pi}}{\alpha L_c} \\
 &\times \exp(-g_b^2/4\alpha^2) I(\alpha, L_c, L_b, g_b) \left. \right] \\
 &- \frac{4\pi}{g^2} e^{-g^2/4\alpha^2} \quad (\text{wire}), \tag{30}
 \end{aligned}$$

where

$$I(\alpha, L_1, L_2, g) = \int_0^{\alpha L_1/2} dx x e^{-g_a^2 L_1^2/16x^2} e^{-x^2} E\left(\frac{2x}{L_1}, L_2, g\right) \tag{31}$$

and

$$E(\lambda, L, g) = \text{erf}\left(\frac{\lambda^2 L + i g}{2\lambda}\right), \tag{32}$$

where $\mathbf{g} = (g_a, g_b, g_c)$ and $g_s = \sqrt{g_a^2 + g_b^2}$. The one-dimensional integrals in Eq. (31) are well suited for using by Gaussian quadrature techniques. It should be noted that a simplified expression for the surface screening function can be obtained in the limit $\alpha \rightarrow \infty$:

$$\bar{\phi}^{(\text{screen})}(\mathbf{g}) = -\frac{4\pi}{g^2} \left[\cos\left(\frac{g_c L_c}{2}\right) e^{-g_s/L_c/2} \right]. \tag{33}$$

However, as is discussed Ref. 54, some care is needed for $g_s = 0$. Similarly, the wire screening function in this limit becomes

$$\begin{aligned}
 \bar{\phi}^{(\text{screen})} \rightarrow & \frac{16}{g^2} \left[\cos\left(\frac{g_b L_b}{2}\right) \frac{J(g_c, g_a, L_c, L_b)}{L_b} \right. \\
 & \left. + \cos\left(\frac{g_c L_c}{2}\right) \frac{J(g_b, g_a, L_b, L_c)}{L_c} \right] - \frac{4\pi}{g^2},
 \end{aligned}$$

TABLE I. Convergence of the total energy for the periodic 8-Si-atom system (see text) for the DVR and PW basis sets. Total energies are in hartrees, and the PW energy cutoff is in Ry. Also given are the number of orbital (N_c) and density (N_{dens}) PW expansion coefficients. The energy difference ($|\Delta E|$) measures the difference between the energy at each grid size/PW cutoff and the converged value in kcal/mol.

Grid size	$E(\text{DVR})$	$ \Delta E $	PW E_{cut}	N_c (N_{dens})	$E(\text{PW})$	$ \Delta E $
16^3	-31.8094	2.4	4	74 (523)	-30.8337	608.7
20^3	-31.8053	0.06	6	126 (968)	-31.2026	376.5
32^3	-31.8052	0	20	752 (6027)	-31.7936	6.3
48^3	-31.8052	0	50	3026 (23917)	-31.8050	0.13
60^3	-31.8052	0	80	6567 (52508)	-31.8051	0.06
64^3 -	-	-	100	8440 (67015)	-31.8052	0

where

$$J(g_1, g_2, L_1, L_2) = \int_0^{L_1/2} dx e^{ig_1 x} \sqrt{\theta(x, g_2, L_2)} \\ \times K_1(\sqrt{4\theta(x, g_2, L_2)}),$$

$$\theta(x, g, L) = \frac{g^2 L^2 / 16}{1 + 4x^2 / L^2},$$

and $K_1(z)$ is a modified Bessel function. Finally, applying Eq. (27) to the Hartree and local pseudopotential energies, the reciprocal-space expressions for these energies become

$$E_{\text{H}} = \frac{1}{V} \sum_{\mathbf{g} \neq 0} |n(\mathbf{g})|^2 \left[\frac{4\pi}{|\mathbf{g}|^2} + \phi^{(\text{screen})}(-\mathbf{g}) \right] \\ + \frac{1}{V} |n(0)|^2 \phi^{(\text{screen})}(0), \quad (34)$$

$$E_{\text{loc}}^{(\text{long})} = \frac{1}{V} \sum_{\mathbf{g}} S(\mathbf{g}) n(\mathbf{g}) [\tilde{V}_{\text{loc}}^{(\text{long})}(-\mathbf{g}) - \phi^{(\text{screen})}(-\mathbf{g})],$$

where the screening function is chosen according to the required boundary conditions.

Other terms that are evaluated in real space via the DVR basis are the short-range component of the local pseudopotential as well as the nonlocal part of the pseudopotential, as discussed in Ref. 61. Finally, we note that for localized orbitals, the coefficient matrix, C_{ijk}^l , is sparse owing to the well-localized nature of the basis functions. It can then be seen that the DVR approach, including the calculation of the

overlap matrix $O_{lm} = \langle \psi_l | \psi_m \rangle = \sum_{i,j,k} C_{ijk}^l C_{ijk}^m$, needed for orthogonalization of the orbitals, will scale inherently as $O(N)$.

III. APPLICATIONS

In order to demonstrate the validity of the DVR approach and compare its convergence with basis set size to the standard PW scheme, we consider a system consisting of 8 silicon atoms in a simple-cubic arrangement in a cubic periodic box of length 5.3 Å. The Kohn-Sham orbitals are expanded about the Γ point, exchange and correlation are treated within the local density approximation, and an atomic pseudopotential⁵⁶ is employed. Table I shows that convergence to within 1 kcal/mol of the total energy with DVR grid size and PW energy cutoff (chosen to give a real-space grid of the same size as the DVR grid) is achieved with a factor of 27 fewer grid points in the DVR basis. The fact that the convergence is not variational reflects the fact that, when a finite basis set is used, the KS Hamiltonian depends on the basis set through its dependence on the orbitals and density. It should be noted that the number of orbital and density coefficients on a 20^3 grid in the DVR case is 8000 in both cases. Given the number of orbital and density expansion coefficients in Table I at an 80 Ry cutoff (which involves an FFT grid of 262 144 points), if the orbitals are not localized, the nonlocal pseudopotential calculation will be about 1.2 times more expensive than that for plane waves, but factors of 33 and 50 are saved in the calculation of the exchange-correlation and Hartree energies, respectively. However, the DVR calculation will generally be dominated by the kinetic energy. Table II shows the convergence of the atomic forces as measured by the quantity

TABLE II. Convergence of atomic forces (see text) in kcal/mol Å for the periodic 8-Si-atom system (see text). $|\Delta \bar{F}|$ measures the difference between the force measure and its converged value.

Grid size	$\bar{F}(\text{DVR})$	$ \Delta \bar{F} $	PW E_{cut}	$\bar{F}(\text{PW})$	$ \Delta \bar{F} $
16^3	13.32	9.37	4	101.49	97.54
20^3	3.92	0.03	6	12.83	8.88
32^3	3.95	0.0	20	3.89	0.06
48^3	3.95	0	50	3.97	0.02
64^3	-	-	100	3.95	0

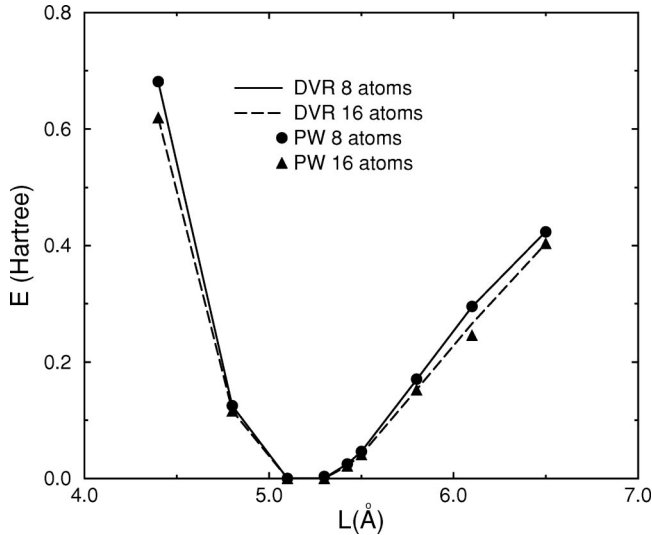


FIG. 1. Energy per unit cell as a function of lattice constant (L) using the DVR approach for an 8-Si-atom system (solid line) and a 16-Si-atom system (dashed line), respectively. The circles and triangles indicate the results from a converged PW calculation on the same system.

$$\bar{\mathbf{F}} = \sqrt{\frac{1}{N} \sum_{I=1}^N \mathbf{F}_I \cdot \mathbf{F}_I}, \quad (35)$$

where \mathbf{F}_I is the force on atom I . The ability to generate accurate forces is of critical importance in AIMD simulations. It can be seen that complete convergence of the forces occurs with a factor of 8 fewer grid points in the DVR basis than in PW basis. Finally, the size consistency of the DVR basis was tested by plotting the energy per unit cell as a function of lattice constant for 8- and 16-atom systems using DVR grid sizes of 20^3 and 40×20^2 , respectively (see Fig. 1). A similar PW control calculation was also performed using a converged basis set size. It can be seen that the energy curves for each system size are very similar and that the DVR and PW results match each other nearly perfectly.

In order to test energy convergence for a large system, a 64-Si-atom system in a diamond lattice was generated. Table III shows the convergence of the total energy per unit cell as in Table I. Again, we see that the DVR result converges with a factor of 25 fewer grid points than the PW result. The

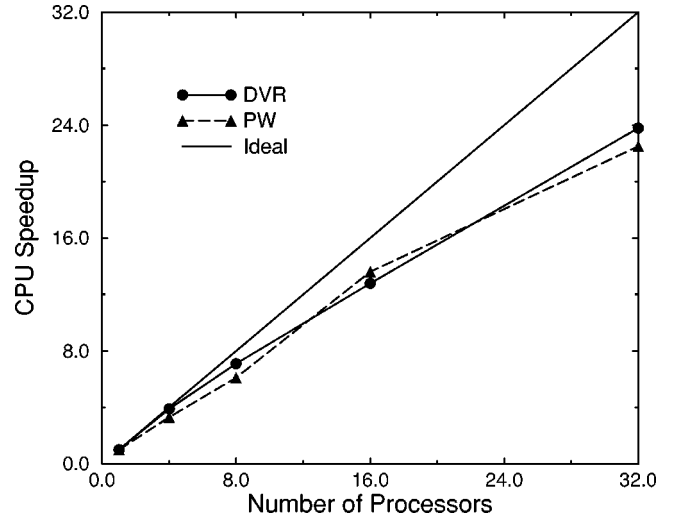


FIG. 2. Parallel scaling of the PW and DVR basis sets for the 64-Si-atom diamond system up to 32 processors.

parallel scaling of the DVR method was also studied. To this end, the DVR method was implemented in parallel in the PINY_MD package developed by the authors.⁶² Although the result is highly dependent on the precise implementation details, a preliminary assessment can be made. Figure 2 shows scaling with the number of processors for the 64-Si-atom system on the terascale system at the Pittsburgh Supercomputing Center. The corresponding PW scaling is also shown. Fully converged calculations, which correspond to 49^3 DVR points and a 120 Ry PW cutoff, are performed for each basis set. It can be seen that the parallel scaling of both methods is comparable. However, the one-processor timing for DVR is roughly one-third that for PW's per step. Although these basis set choices give exactly the same converged total energy, a PW cutoff of 100 Ry is very close to the 120 Ry result. The one-processor timing for the DVR calculation is roughly one-half that of a 100 Ry PW calculation. Finally, a 256-Si-atom system was studied for timing purposes on a local parallel machine with 16 processors. With a cutoff of 120 Ry, the PW calculation just fits, while a converged DVR calculation with a $49 \times 98 \times 98$ grid size easily fits and requires one-third the CPU time of PW's per step. Similarly the DVR calculation requires one-half the CPU time of a 100 Ry PW

TABLE III. Convergence of the total energy per unit cell for a periodic 64-Si-atom system in a diamond lattice (see text) for the DVR and PW basis sets. Total energies are in hartrees, and the PW energy cutoff is in Ry. Also given are the number of orbital (N_c) and density (N_{dens}) PW expansion coefficients. The energy difference ($|\Delta E|$) measures the difference between the energy at each grid size/PW cutoff and the converged value in kcal/mol.

Grid size	$E(\text{DVR})$	$ \Delta E $	PW E_{cut}	N_c (N_{dens})	$E(\text{PW})$	$ \Delta E $
29^3	-31.6460	1.5	4	484 (3 671)	-31.0803	353.5
33^3	-31.6438	0.1	5	752 (6 027)	-31.2467	249.0
39^3	-31.6437	0.06	7	1 259 (10 003)	-31.4108	146.0
49^3	-31.6436	0	12	2 788 (22 513)	-31.5793	40.3
80^3	-	-	40	17 070 (135 555)	-31.6132	19.1
144^3	-	-	120	88 755 (710 378)	-31.6436	0

TABLE IV. Convergence of total energy for one H₂O molecule cluster system in a 5 Å box for the DVR and PW basis sets. Total energies are in hartrees, and the PW energy cutoff is in Ry. Also given are the number of orbital (N_c) and density (N_{dens}) PW coefficients. The energy difference $|\Delta E|$ measures the difference between the energy at each grid size/PW cutoff and the converged energy in kcal/mol.

Grid size	$E(\text{DVR})$	$ \Delta E $	PW E_{cut}	$N_c(N_{\text{dens}})$	$E(\text{PW})$	$ \Delta E $
24 ³	-17.1222	45.6200	10	231 (1 848)	-15.1056	1311.0566
32 ³	-17.1769	11.2952	20	656 (5 066)	-16.0058	746.1721
40 ³	-17.1939	0.6275	40	1 848 (14 333)	-16.8569	212.0984
48 ³	-17.1948	0.0627	50	2 521 (10 270)	-17.0183	110.8183
60 ³	-17.1949	0	80	5 066 (40 657)	-17.1776	10.8559
80 ³	-	-	180	17 166 (136 191)	-17.1938	0.6903
108 ³	-	-	300	37 063 (295 945)	-17.1949	0

calculation. Note, however, that such timings will change when the DVR is used in conjunction with localized orbitals.

As an illustration of the use of the DVR basis in conjunction with a generalized gradient exchange and correlation functional and cluster boundary conditions, we consider a single water molecule in a 5 Å cubic box. Exchange and correlation are treated using the Becke–Lee–Yang–Parr (BLYP) functional,^{63,64} and atomic pseudopotentials⁵⁷ are employed. In this case, long-range terms are treated using the cluster form of the reciprocal-space screening function. Here, it is found that the energy is converged to within 1 kcal/mol of the fully converged value (-17.1949 hartrees) with a grid size of 40³ points whereas a PW grid size of 80³ points is required (see Table IV). In the latter case, this corresponds to a PW energy cutoff of 180 Ry. Note that 40³ would correspond to a PW cutoff of 40 Ry. AIMD simulations of water are usually performed in the PW basis using a cutoff of 70–80 Ry, where the total energy is still more than 10 kcal/mol different from the fully converged value. Nearly full convergence is achieved on a 48³ grid for the DVR basis and a 108³ grid for the PW basis. In the latter case, this corresponds to a PW energy cutoff of 300 Ry.

Finally, in order to illustrate the utility of the DVR approach in AIMD calculations, we consider, once again, the periodic 8-silicon-atom system described above. The general AIMD scheme is based on a Car-Parrinello¹ type of adiabatic equations of motion:

$$\mu \ddot{C}_{ijk}^l = -\frac{\partial E}{\partial C_{ijk}^l} + \sum_m \Lambda_{lm} C_{ijk}^m,$$

$$M_l \ddot{\mathbf{R}}_l = -\frac{\partial E}{\partial \mathbf{R}_l}, \quad (36)$$

in which a fictitious electronic dynamics is used to generate the approximate instantaneous ground-state electronic configuration at each nuclear configuration in a molecular dynamics run. Here, E is given by Eq. (9), and Λ_{lm} is a set of Lagrange multipliers for enforcing the orthogonality condition, and μ is chosen to ensure an adiabatic separation between the nuclear and fictitious electronic degrees of freedom. A short Car-Parrinello molecular dynamics run is performed using a time step of 0.125 fs on a 20³ grid. Core

electrons are treated using an atomic pseudopotential.⁵⁶ Figures 3(a) and 3(b) show that the fictitious electronic kinetic energy is stable and small compared to the ionic kinetic energy, indicating that adiabaticity is well maintained in the DVR basis.

IV. CONCLUSIONS

A simple, rigorous, and efficient real-space approach to electronic structure calculations for use in AIMD calculations has been introduced. The method is based on the use of a discrete variable representation basis set and a unified reciprocal-space treatment of long-range interactions and can therefore treat systems with zero-, one-, two-, and three-dimensional periodicity within a single framework. This approach has been shown to converge faster with grid size than the widely used PW approach and to yield a stable Car-Parrinello-type AIMD scheme. We are currently developing an approach⁶⁵ that exploits the Car-Parrinello dynamics to

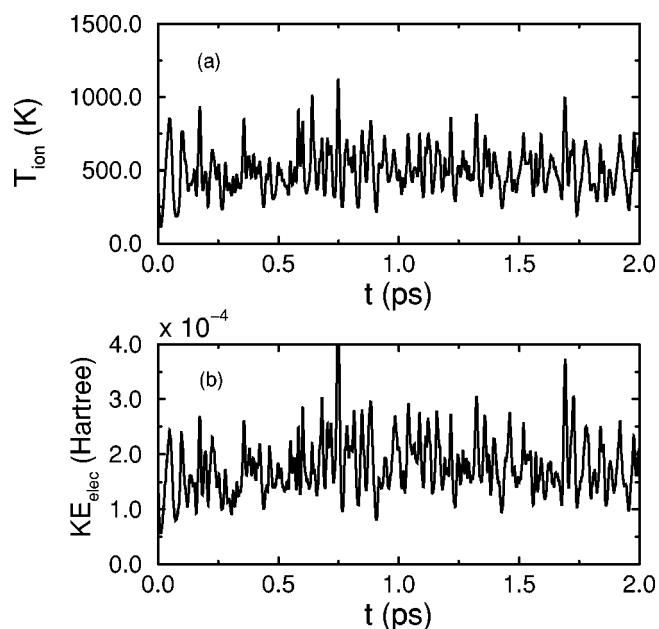


FIG. 3. (a) Instantaneous value of the fictitious electronic kinetic energy (in hartrees) over a 2 ps Car-Parrinello AIMD run for the 8-Si-atom system. (b) Instantaneous value of the ionic kinetic energy (in kelvin) over a 2 ps Car-Parrinello AIMD run.

give an “on the fly” orbital localization scheme that will be combined with the DVR approach to give a linear scaling method. Through such developments, we hope to significantly extend the capabilities of AIMD calculations in the near future.

ACKNOWLEDGMENTS

This research was supported by Research Corp. Grant No. RI0218, NSF Grant No. CHE-9875824, and NSF Grant No. CHE-0121375.

- ¹R. Car and M. Parrinello, *Phys. Rev. Lett.* **55**, 2471 (1985).
- ²G. Galli and M. Parrinello, in *Computer Simulation for Chemical Physics*, Vol. 397 of *NATO Advanced Study Institute, Series C: Mathematical and Physical Sciences*, edited by M.P. Allen and D.J. Tildesley (Kluwer, 1993), p. 261.
- ³D.K. Remler and P.A. Madden, *Mol. Phys.* **70**, 921 (1990).
- ⁴M.C. Payne, M.P. Teter, D.C. Allan, T.A. Arias, and J.D. Joannopoulos, *Rev. Mod. Phys.* **64**, 1045 (1992).
- ⁵D. Marx and J. Hutter, in *Modern Methods and Algorithms of Quantum Chemistry*, edited by J. Grotendorst (John von Neumann Institute for Computing, Forschungszentrum, Juelich, 2000), NIC Series Vol. 1, pp. 301–449.
- ⁶M.E. Tuckerman, *J. Phys.: Condens. Matter* **14**, R1297 (2002).
- ⁷J. Aqvist and A. Warshel, *Chem. Rev. (Washington, D.C.)* **93**, 2523 (1993).
- ⁸G. Monard, M. Loos, V. Thery, K. Baka, and J.L. Rivail, *Int. J. Quantum Chem.* **58**, 153 (1996).
- ⁹J. Bentzien, R.P. Muller, J. Florian, and A. Warshel, *J. Phys. Chem. B* **102**, 2293 (1998).
- ¹⁰Y.K. Zhang, T.S. Lee, and W.T. Yang, *J. Chem. Phys.* **110**, 46 (1999).
- ¹¹N. Reuter, A. Dejaegere, B. Maigret, and M. Karplus, *J. Phys. Chem. A* **104**, 1720 (2000).
- ¹²D.A. Yarne, M.E. Tuckerman, and G.J. Martyna, *J. Chem. Phys.* **115**, 3531 (2001).
- ¹³A. Laio, J. VandeVondele, and U. Rothlisberger, *J. Chem. Phys.* **116**, 6941 (2002).
- ¹⁴S.R. White, J.W. Wilkins, and M.P. Teter, *Phys. Rev. B* **39**, 5819 (1989).
- ¹⁵B. Hartke and E.A. Carter, *Chem. Phys. Lett.* **189**, 358 (1992).
- ¹⁶J. Ackermann and R. Roitzsch, *Chem. Phys. Lett.* **214**, 109 (1993).
- ¹⁷J.R. Chelikowsky, N. Troullier, and Y. Saad, *Phys. Rev. Lett.* **72**, 1240 (1994).
- ¹⁸F. Gygi and G. Galli, *Phys. Rev. B* **52**, R2229 (1995).
- ¹⁹E.L. Briggs, D.J. Sullivan, and J. Bernholc, *Phys. Rev. B* **52**, R5471 (1995).
- ²⁰E.L. Briggs, D.J. Sullivan, and J. Bernholc, *Phys. Rev. B* **54**, 14362 (1996).
- ²¹E. Tsuchida and M. Tsukada, *Phys. Rev. B* **54**, 7602 (1996).
- ²²G. Lippert, J. Hutter, and M. Parrinello, *Mol. Phys.* **92**, 477 (1997).
- ²³G. Lippert, J. Hutter, and M. Parrinello, *Theor. Chem. Acc.* **103**, 124 (1998).
- ²⁴M. Krack and M. Parrinello, *Phys. Chem. Chem. Phys.* **2**, 2105 (2000).
- ²⁵T.L. Beck, *Rev. Mod. Phys.* **72**, 1041 (2000).
- ²⁶H.B. Schlegel, J.M. Millam, S.S. Iyengar, G.A. Voth, A.D. Daniels, G.E. Scuseria, and M.J. Frisch, *J. Chem. Phys.* **114**, 9758 (2001).
- ²⁷F. Shimojo, R.K. Kalia, A. Nakano, and P. Vashishta, *Comput. Phys. Commun.* **140**, 303 (2001).
- ²⁸P.K. Venkatesh, *Physica B* **318**, 121 (2002).
- ²⁹N. Cholý and E. Kaxiras, *Phys. Rev. B* **67**, 155101 (2003).
- ³⁰J.C. Light, I.P. Hamilton, and J.V. Lill, *J. Chem. Phys.* **82**, 1400 (1985).
- ³¹R.A. Friesner, *Chem. Phys. Lett.* **116**, 39 (1985).
- ³²Z. Bačić and J.C. Light, *Annu. Rev. Phys. Chem.* **40**, 469 (1989).
- ³³S.E. Choi and J.C. Light, *J. Chem. Phys.* **90**, 2593 (1989).
- ³⁴J.T. Muckerman, *Chem. Phys. Lett.* **173**, 200 (1990).
- ³⁵D.T. Colbert and W.H. Miller, *J. Chem. Phys.* **96**, 1982 (1992).
- ³⁶S. Guerin and H.R. Jauslin, *Comput. Phys. Commun.* **121-122**, 496 (1999).
- ³⁷J.C. Light and T. Carrington, *Adv. Chem. Phys.* **114**, 263 (2000).
- ³⁸R.G. Littlejohn and M. Cargo, *J. Chem. Phys.* **117**, 27 (2002).
- ³⁹R.G. Littlejohn and M. Cargo, *J. Chem. Phys.* **117**, 37 (2002).
- ⁴⁰M. Cargo and R.G. Littlejohn, *J. Chem. Phys.* **117**, 59 (2002).
- ⁴¹R.G. Littlejohn *et al.*, *J. Chem. Phys.* **116**, 8691 (2002).
- ⁴²D.G. Pettifor, *Phys. Rev. Lett.* **63**, 2480 (1989).
- ⁴³W. Yang, *Phys. Rev. Lett.* **66**, 1438 (1991).
- ⁴⁴G. Galli and M. Parrinello, *Phys. Rev. Lett.* **69**, 3547 (1992).
- ⁴⁵M.S. Daw, *Phys. Rev. B* **47**, 10 895 (1993).
- ⁴⁶F. Mauri, G. Galli, and R. Car, *Phys. Rev. B* **47**, 9973 (1993).
- ⁴⁷X.P. Li, R.W. Nunes, and D. Vanderbilt, *Phys. Rev. B* **47**, 10891 (1993).
- ⁴⁸P. Ordejon, D.A. Drabold, M.P. Grumbach, and R.M. Martin, *Phys. Rev. B* **48**, 14646 (1993).
- ⁴⁹M. Aoki, *Phys. Rev. Lett.* **71**, 3842 (1993).
- ⁵⁰S. Goedecker, *Rev. Mod. Phys.* **71**, 1085 (1999).
- ⁵¹D.R. Bowler, T. Miyazaki, and M.J. Gillan, *J. Phys.: Condens. Matter* **14**, 2781 (2002).
- ⁵²Z. Bačić and J.C. Light, *J. Chem. Phys.* **85**, 4594 (1986).
- ⁵³G. Martyna and M. Tuckerman, *J. Chem. Phys.* **110**, 2810 (1999).
- ⁵⁴P. Minary, M.E. Tuckerman, K.A. Pihakari, and G.J. Martyna, *J. Chem. Phys.* **116**, 5351 (2002).
- ⁵⁵M.E. Tuckerman, P. Minary, K.A. Pihakari, and G.J. Martyna, in *Computational Methods for Macromolecules: Challenges and Applications*, edited by T. Schlick and H.H. Gan (Springer, Berlin, 2002), p. 381.
- ⁵⁶G.B. Bachelet, D.R. Hamann, and M. Schlüter, *Phys. Rev. B* **26**, 4199 (1982).
- ⁵⁷N. Troullier and J.L. Martins, *Phys. Rev. B* **43**, 1993 (1991).
- ⁵⁸J.A. White and D.M. Bird, *Phys. Rev. B* **50**, 4954 (1994).
- ⁵⁹L. Greengard and V. Rokhlin, *Chem. Scr.* **29A**, 139 (1989).
- ⁶⁰C. White and M. Head-Gordon, *J. Chem. Phys.* **101**, 6593 (1994).
- ⁶¹M.E. Tuckerman and M. Parrinello, *J. Chem. Phys.* **101**, 1316 (1994).
- ⁶²M.E. Tuckerman, D.A. Yarne, S.O. Samuelson, A.L. Hughes, and G.J. Martyna, *Comput. Phys. Commun.* **128**, 333 (2000).
- ⁶³A.D. Becke, *Phys. Rev. A* **38**, 3098 (1988).
- ⁶⁴C. Lee, W. Yang, and R.G. Parr, *Phys. Rev. B* **37**, 785 (1988).
- ⁶⁵J.W. Thomas, R. Iftimie, and M.E. Tuckerman (unpublished).
- ⁶⁶J.A. Morrone, P. Minary, and M.E. Tuckerman (unpublished).